CHEMICAL ENGINEERING TRANSACTIONS
VOL. 81, 2020
A publication of AIDIC
The Italian Association of Chemical Engineering
Online at www.cetjournal.it
Guest Editors: Petar S. Varbanov, Qiuwang Wang, Min Zeng, Panos Seferlis, Ting Ma, Jiří J. Klemeš

ISBN 978-88-95608-79-2; **ISSN** 2283-9216
DOI: 10.3303/CET2081088

Investigate the Thermal Performance of Thermocline Tank for Hybrid Solar Tower Power Plants

Karem Elsayed Elfeky, Abubakar Gambo Mohammed, Qiuwang Wang*

Key Laboratory of Thermo-Fluid Science and Engineering, MOE, Xi'an Jiaotong University, Xi'an, Shaanxi 710049, China
wangqw@mail.xjtu.edu.cn

Solar tower power (STP) plants integrated with thermal energy storage (TES) subsystems are expected to be a potential solution to meet the world's future energy needs. Air rock bed TES subsystem emphasizes to be efficient and cheap storage for STP plants. In the present study, the discrete element method (DEM) coupled with the computational fluid dynamics (CFD) model are adopted to study the fluid flow and heat transfer process of an air rock thermocline TES tank. The study is carried out to investigate the thermal behaviour of the TES thermocline tank by changing the Reynolds number. The results show that the temperature difference between both the heat transfer fluid (HTF) and the spheres for charging cycle decreases with increasing of the Reynolds number, but also the total rate of heat transfer increases. The results illustrated that the difference in temperature between the HTF and the spheres for discharging cycle decreases with increase in the Reynolds number and this difference in temperature is less during the discharging cycle than the charging cycle. In addition, the Re = 1,200 case exhibit the optimized behaviour as it possesses the higher matching in temperature distributions of spheres with the temperature profiles of HTF. The Re = 400 shows reduced charging/discharging performance as the low rate of heat transfer between spheres and HTF.

1. Introduction

Solar energy is the best sources of energy expected to meet the world's energy requirements, reduce fuel prices and prevent the increase of greenhouse gases emission (Pizzolato et al., 2016). The intermittent nature of solar energy needs an energy storage subsystem to use the energy source effectively. The technologies of solar thermal energy, such as solar tower power (STP) plants; capture the thermal energy of the sun and convert it into electrical power by a heat engine connected with a generator (Pramanik and Ravikrishna, 2017). One of the most significant features of STP technology is its ability to store energy efficiently and at low cost (Li and Ju, 2018). The thermal energy storage (TES) subsystem in an air rock thermocline TES tank is efficient and reasonable storage for STP plants (Hoivik et al., 2019).

More recently, the subject of TES using bed rocks has been of interest to researchers. The most important properties of storage materials are the heat capacity and the conductivity, but the conductivity has less effect (Hänchen et al., 2011). The thermal behaviour of the TES thermocline tank has been investigated to know how to improve the heat transfer process during the charging/discharging cycles (Elfeky et al., 2018). Rao et al. (2019) presented the performance investigation of three lab-scale solid sensible heat storage prototypes. In similar work, Tiskatine et al. (2017) studied the effect of the axial porosity variation and how to select convenient storage medium for packed bed TES subsystem and compared the results with 3-D CFD simulations. The first researchers who conduct a study to determine the coefficient of heat transfer in a porous medium filled with rocks (Löf et al., 1984). The results illustrated that the rate of heat transfer depends on the mass flux and the particle size, while the inlet temperature has no obvious effect. The thermal performance of a 1 MWe STP plants has been investigated using direct and indirect TES subsystems by Cocco et al. (2015).

Based on the above literature review, it can be noted that most of the previous numerical studies lack clear knowledge for the process of the heat transfer between the HTF and the filler material in detail, e.g., influence of the Reynolds number on the amount of increasing/decreasing the temperature of the filler material for the charging/discharging cycles in the axial direction and the influence of the Reynolds number on the absorb and

Paper Received: 01/03/2020; Revised: 09/04/2020; Accepted: 12/04/2020
Please cite this article as: Elfeky K.E., Mohammed A.G., Wang Q., 2020, Investigate the Thermal Performance of Thermocline Tank for Hybrid Solar Tower Power Plants, Chemical Engineering Transactions, 81, 523-528 DOI:10.3303/CET2081088

recover thermal energy, especially at low Reynolds number during charging/discharging cycles. In the present study, the thermal performance of the random packed bed for thermocline TES tank is numerically investigated a different Reynolds number for the charging/discharging cycles.

2. Model formulation

2.1 Physical model

Packed bed TES subsystems have proven its effectiveness in the thermal storage process because of its high heat transfer rate during the charging/discharging cycles. Figure 1 schematically shows the structure of the thermocline TES tank. The aspect ratio (H_{tank}/D_{bed}) of the tank is 4.287, comparable to that used in STP applications (Zanganeh et al., 2015). During the charging cycle, the hot HTF at temperature T_h passing from the top part of the tank. During the discharging cycle, the cold HTF passing from the bottom part of the tank at temperature T_c. The packed bed region height is indicated by H_{bed}, while D_{bed} indicated the diameter of the tank. The thermocline TES tank is filled with 515 spheres at average porosity of ϕ, which is mentioned in Table 1 . The geometrical parameters of the packing models are presented in Table 1.

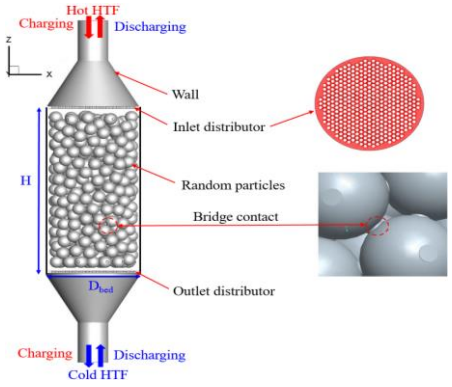

Figure 1: Schematic diagram of physical model of the thermocline TES tank

Table 1: Geometrical parameters of thermocline TES tank

Parameters	Values	Parameters	Values
H_{tank} (m)	0.171	d_s (m)	0.006
H_{bed} (m)	0.08	T_h (°C)	650
D_{bed} (m)	0.04	T_c (°C)	350
ϕ (-)	0.417	HTF	Air

In the present study, the DEM method is employed to generate 515 spheres (Bai et al.,2009). Using EDEM program (DEM Solutions Ltd., 2016), the solid spherical particles are fallen to the bottom of the tank by gravity. The particle data (diameter and position of the centroid) of the finished DEM simulation will export after that this data will import into a Pro/ENGINEER Wildfire (Tickoo, 2010). The last step, the resulting CAD geometry is then will export and import into the CFD program ICEM for meshing and calculating.

2.2 Governing equations and computational methods

In this study, the fluid flow is unsteady and incompressible in order to simulate real operating conditions of TES tank. The three-dimensional Navier-Stokes and energy equations are applied. The particle Reynolds number (Re_p) is changing from 400 to 1,600. The RNG k-ε turbulence model is recommended to study the turbulent flow in the porous medium, especially for small-scale eddies that are independent of larger phenomena (Yang et al., 2010). The equations of conservation for mass, momentum, and energy are presented as:
Continuity:

$$\frac{\partial \rho}{\partial t} + \rho(\nabla \cdot \vec{V}) = 0 \tag{1}$$

Momentum:

$$\rho_f\left[\frac{\partial \vec{V}}{\partial t}+(\vec{V}\cdot\nabla\vec{V})\right]=\rho g-\nabla p+\nabla\cdot[(\mu_f+\mu_t)(\nabla\vec{V}+(\nabla\vec{V})^T)] \quad (2)$$

Energy:

$$\rho_f\left[\frac{\partial T}{\partial t}+(\vec{V}.\nabla T)\right]=\nabla\cdot[(\frac{k_f}{c_p}+\frac{\mu_t}{\sigma_T})\cdot(\nabla T)] \quad (3)$$

The RNG k-ε model transport equations are presented as:

$$k:\rho_f\left[\frac{\partial k}{\partial t}+(\vec{V}.\nabla k)\right]=\nabla\cdot[(\mu_f+\frac{\mu_t}{\sigma_k})\cdot\nabla k]+P_k-\rho_f\varepsilon \quad (4)$$

$$\varepsilon:\rho_f\left[\frac{\partial \varepsilon}{\partial t}+(\vec{V}.\nabla \varepsilon)\right]=\nabla\cdot[(\mu_f+\frac{\mu_t}{\sigma_\varepsilon})\cdot\nabla\varepsilon]+\frac{c_{\varepsilon 1}\varepsilon}{k}P_k-c_{\varepsilon 2}\rho_f\frac{\varepsilon^2}{k} \quad (5)$$

where P_k is the turbulence shear production, μ_t is the turbulent viscosity, $c_{\varepsilon 1}$and $c_{\varepsilon 2}$ are constants of the turbulence model in ε equation, σ_T, σ_k and σ_ε are the Prandtl numbers in T, k and ε equations. The values of these constants are presented as:

$$P_k=\mu_t\cdot(\nabla\vec{V}+(\nabla\vec{V})^T):\nabla\vec{V};\ \ \mu_t=\rho_f c_\mu\frac{k^2}{\varepsilon}\ \ (c_\mu=0.085) \quad (6)$$

$$c_{\varepsilon 1}=1.42-f_\eta\ \ (f_\eta=\frac{\eta(1-\eta/4.38)}{1+0.012\eta^3},\ \ \eta=\frac{P_k}{\rho_f c_\mu\varepsilon}) \quad (7)$$

where $c_{\varepsilon 2}$, σ_T, σ_k and σ_ε are equal 1.68, 1.0, 0.718, 0718.
The commercial code of ANSYS FLUENT 16.0 (ANSYS Inc., 2015) is applied in this study to solve the continuity, momentum and energy equations. To couple the velocities and pressure in the equations of conservation, the SIMPLE algorithm is used. The second-order upwind scheme is applied to discretize the convective terms in the momentum, energy and turbulence equations.

2.3 Mesh generation and grid independence test

The geometry of the thermocline TES tank with 515 spheres is very complicated. In the present work, the geometric model is divided using tetrahedral mesh. Short cylinder bridges are created in order to modify the mesh at the points of contact as shown in Figure 2a. This modification is carried out according to a study conducted by (Dixon et al., 2012). A thermocline TES tank with 70 spheres (H_{bed} = 0.08 m, D_{bed}/d_s = 5 and d_s = 0.008 m) was created to determine the size of the appropriate computational element. The changes of Nusselt numbers and drag coefficients with the sizes of the computational element are shown in Figure 2b. The results showed that the grid size effect on the drag coefficient and the Nusselt number will be ineffective when the size of the computational element is less than 1/20 d_s.

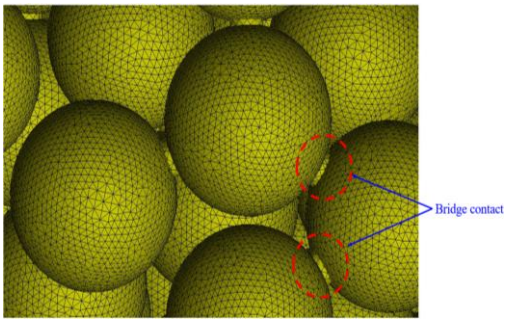

(a)

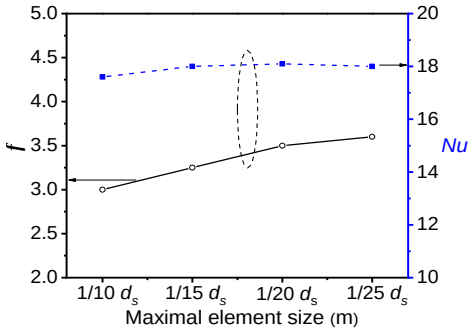

(b)

Figure 2: Thermocline TES tank: (a) Computational mesh and (b) Variations of drag coefficients and Nusselt numbers with different mesh element size

3. Results and discussion

In the present work, the thermal behavior of the TES thermocline tank is one of the important parameters for determining the power generation and the STP efficiency. The process of TES in the thermocline tank keeps the STP plants in operation, the heat transfer process inside this tank during the charging/discharging cycles is of fundamental importance and will be studied in detail in this research.

3.1 Axial temperature distribution for charging/discharging cycles

Figure 3 shows the HTF and spheres axial temperature distribution at different Reynolds number for charging process. The driving force for forced convection is the difference between HTF and spheres temperature, which leads to the thermal flux as function of temperature difference. It is obvious that there is a strong nonuniformity in temperature distribution for the random packed bed at different Reynolds number. At Re = 400, average temperature of HTF and spheres are 445.83 °C and 378.92 °C. At Re = 800, average temperature of HTF and spheres are 476.92 °C and 413.03 °C. At Re = 1,200, average temperature of HTF and spheres are 504.24 °C and 444.89 °C. At Re = 1,600, average temperature of HTF and spheres are 527.47 oC and 472.4 °C.

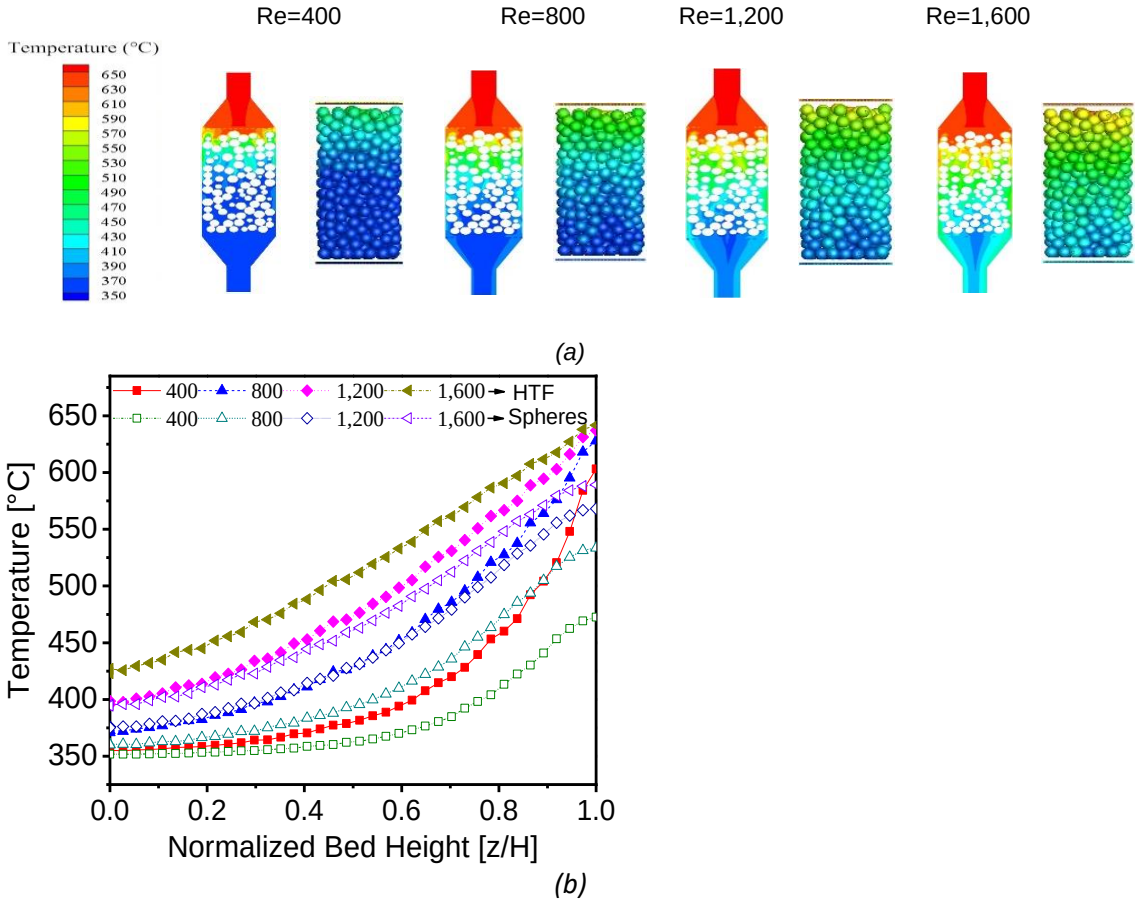

Figure 3: Temperature of the packed bed for charging cycle after 175 s: (a) HTF /spheres axial temperature contours and (b) HTF/spheres axial temperatures profile

Figure 4 shows the HTF and spheres axial temperature distribution at different Reynolds number for discharging process. There is very little declining stage at the starting of the discharging cycle and the fast change in temperature difference appears much earlier in discharging than in the charging cycle. From Figure 4a and b, it can be observed that the temperature drop occurs quickly when the Reynolds number increases. This can mostly be attributed to the enhancement of the rate of heat transfer. The difference in temperature between the HTF and the spheres changes as follows: ΔT = 41.0 °C at Re = 400, ΔT = 17.2 °C at Re = 800, ΔT = 12.6 °C at Re = 1,200 and ΔT = 8.5 °C at Re = 1,600. The above results can be summarized as the difference in temperature between both the spheres and the HTF during the discharging cycle decreases with increase in

the Reynolds number and this difference in temperature is less during the discharging cycle than the charging cycle.

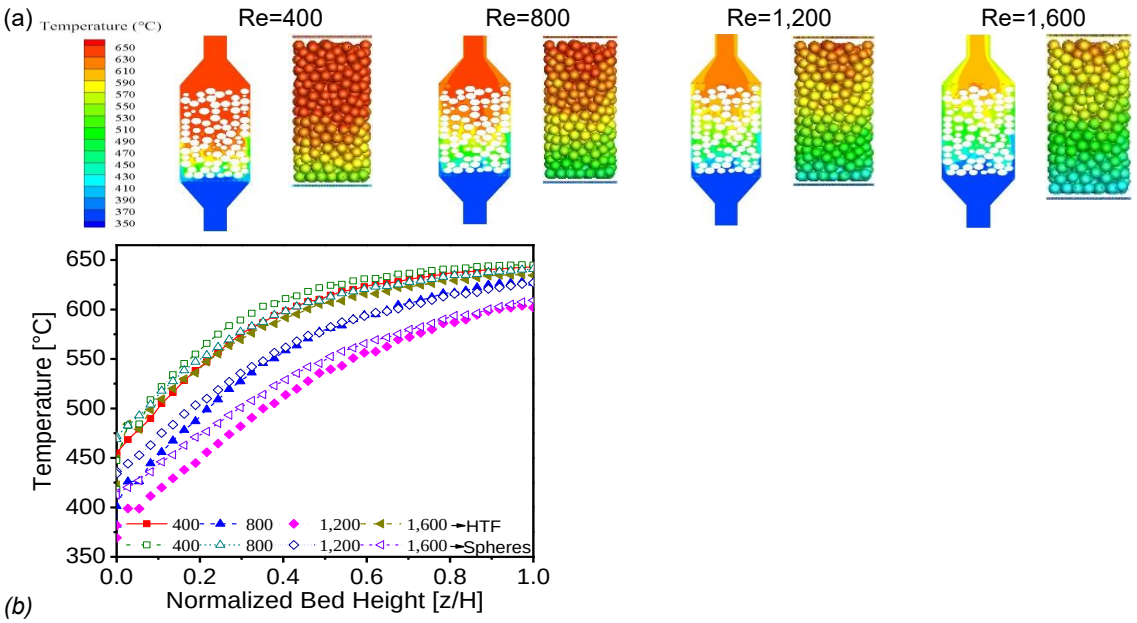

Figure 4: Temperature of the packed bed for discharging cycle after 175 s: (a) HTF /spheres axial temperature contours and (b) HTF/spheres axial temperatures profile

3.2 Storage capacity

The performances of the thermocline TES tank are presented as a function of the total amount of energy transferred for the charging cycle and the amount of energy recovered during the discharging cycle as demonstrated in Figure 5a and b. Total energy transfers to or from the spherical particles determined the performance of the tank, and the large difference in temperature between the hot charging/discharging HTF and the sphere's temperature gives a large driving force for the heat transfer process, promote rapid movement of thermal zones. The graph shows that the Re = 1,600 achieves the fastest storage or recover in the least time period, Re = 1,200 the second, Re = 800 the third and Re = 400 is the lowest in the row. The Re = 1,200 case exhibit the optimized behavior as it possesses the higher matching in temperature distributions of spheres with the temperature profiles of HTF.

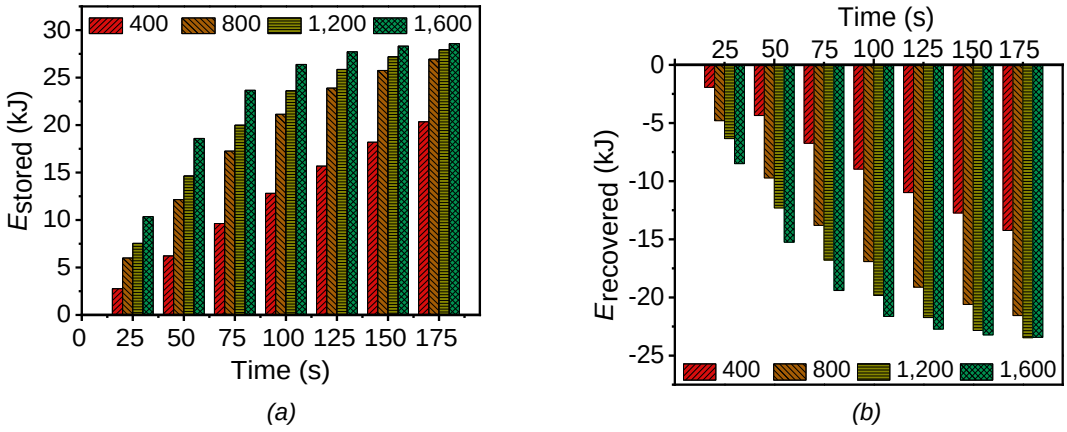

Figure 5: Total energy stored and released in the thermocline tank vs. time for different inlet Reynolds number during (a) charging cycle (b) discharge cycle

4. Conclusions

In the present work, the DEM coupled with the CFD model are adopted to study the fluid flow and heat transfer process of an air rock thermocline TES tank. The study is carried out to investigate the thermal behaviour of the TES thermocline tank by changing the Reynolds number. The results show that the temperature difference between both the HTF and the spheres for charging cycle decreases with increasing of the Reynolds number, but also the total rate of heat transfer increases. The results illustrated that the difference in temperature between the HTF and the spheres for discharging cycle decreases with increase in the Reynolds. In addition, the Re = 1,200 case exhibit the optimized behaviour as it possesses the higher matching in temperature distributions of spheres with the temperature profiles of HTF. This work can be extended by investigating the charging/discharging efficiency, overall efficiency, capacity ratio, and utilization ratio of the air rock thermocline thermal energy storage tank to optimize it's thermal performance which used in solar tower power plants.

Acknowledgments

This work is financially supported by the National Natural Science Foundation of China (Grant No. 51536007) and the 111 Project (B16038).

References

ANSYS Inc., 2015, ANSYS Fluent User's Guide, Release 16.0, Ansys Inc., Canonsburg, PA, USA.

Bai H., Theuerkauf J., Gillis P.A., Witt P.M., 2009, A coupled DEM and CFD simulation of flow field and pressure drop in fixed bed reactor with randomly packed catalyst particles, Industrial & Engineering Chemistry Research, 48, 4060-4074.

Cocco D., Serra F., 2015, Performance comparison of two-tank direct and thermocline thermal energy storage systems for 1 MWe class concentrating solar power plants, Energy, 81, 526-536.

Chandra P., Willits D.H., 1981, Pressure drop and heat transfer characteristics of air-rock bed thermal storage systems, Solar Energy, 27, 547-553.

DEM Solutions Ltd., 2016, EDEM 2017 User Guide, <www.edemsimulation.com/content/uploads/2016/08/Referencing_Guidelines_for_EDEM_Users_2016.pdf>, accessed 23.05.2020.

Dixon A.G., Walls G., Stanness H., Nijemeisland M., Stitt E.H., 2012, Experimental validation of high Reynolds number CFD simulations of heat transfer in a pilot-scale fixed bed tube, Chemical Engineering Journal, 200, 344-356.

Elfeky K.E., Ahmed N., Wang Q., 2018, Numerical comparison between single PCM and multi-stage PCM based high temperature thermal energy storage for CSP tower plants, Applied Thermal Engineering, 139, 609-622.

Hänchen M., Brückner S., Steinfeld A., 2011, High-temperature thermal storage using a packed bed of rocks-heat transfer analysis and experimental validation, Applied Thermal Engineering, 31, 1798-1806.

Hoivik N., Greiner C., Barragan J., Iniesta A.C., Skeie G., Bergan P., Blanco-Rodriguez P., Calvet N., 2019, Long-term performance results of concrete-based modular thermal energy storage system, Journal of Energy Storage, 24, 100735.

Li B., Ju F., 2018, Thermal stability of granite for high temperature thermal energy storage in concentrating solar power plants, Applied Thermal Engineering, 138, 409-416.

Löf G.O.G., Hawley R.W., 1948, Unsteady-state heat transfer between air and lose solids, Industrial Chemical Engineering, 40, 1061-1070.

Pizzolato A., Donato F., Verda V., Santarelli M., Sciacovelli A., 2017, CSP plants with thermocline thermal energy storage and integrated steam generator-Techno-economic modeling and design optimization, Energy, 139, 231-246.

Pramanik S., Ravikrishna R.V., 2017, A review of concentrated solar power hybrid technologies, Applied Thermal Engineering, 127, 602-637.

Rao C.R.C., Vigneshwaran K., Niyas H., Muthukumar P., 2019, Performance investigation of lab-scale sensible heat storage prototypes, International Journal of Green Energy, 16(14), 1363-1378.

Tiskatine R., Aharoune A., Bouirden L., Ihlal A., 2017, Identification of suitable storage materials for solar thermal power plant using selection methodology, Applied Thermal Engineering, 117, 591-608.

Tickoo S., 2010. Pro/ENGINEER Wildfire 5.0 for Designers Textbook: CADCIM Technologies, Schererville, IN, USA.

Yang J., Wang Q., Zeng M., Nakayama A., 2010, Computational study of forced convective heat transfer in structured packed beds with spherical or ellipsoidal particles, Chemical Engineering Science, 65, 26-738.

Zanganeh G., Khanna R., Walser C., Pedretti A., Haselbacher A., Steinfeld A., 2015, Experimental and numerical investigation of combined sensible–latent heat for thermal energy storage at 575 °C and above, Solar Energy, 114, 77-90.